Double-Miniemulsion Preparation of Fe_3O_4/Poly(methyl methacrylate) Magnetic Latex

R. Y. Hong,[1,2] B. Feng,[1] X. Cai,[1] G. Liu,[1] H. Z. Li,[2] J. Ding,[3] Y. Zheng,[4] D. G. Wei[5]

[1]*College of Chemical Engineering and Materials Science & Key Laboratory of Organic Synthesis of Jiangsu Province, Soochow University, Suzhou 215123, China*
[2]*State Key Laboratory of Multiphase Reaction, Institute of Process Engineering, Chinese Academy of Sciences, Beijing 100080, China*
[3]*IBM, HYDA/050-3 C202, 3605 Highway 52 North, Rochester, Minnesota 55901*
[4]*Department of Chemical Engineering, University of New Brunswick, Fredericton, N.B. E3B 5A3, Canada*
[5]*Center for Nanoscale Systems, School of Engineering & Applied Sciences, Harvard University, Cambridge, Massachusetts 02139*

Received 1 December 2007; accepted 4 September 2008
DOI 10.1002/app.29403
Published online 22 December 2008 in Wiley InterScience (www.interscience.wiley.com).

ABSTRACT: Magnetic poly(methyl methacrylate) (PMMA) microspheres were prepared by double-miniemulsion polymerization. First, oleic acid coated magnetite particles synthesized by means of coprecipitation were dispersed into octane to obtain a ferrofluid. The ferrofluid and MMA were emulsified to form O/W emulsion, respectively. Subsequently two miniemulsions were mixed together for polymerization. The obtained magnetic polymer particles were characterized by Fourier transform infrared spectroscopy, transmission electron microscopy, scanning electron microscopy, X-ray powder diffraction, and thermogravimetry. The results showed that oleic acid coated magnetite particles were well encapsulated in PMMA. The effects of initiator dosage and monomer concentration on the conversion of MMA were also investigated. © 2008 Wiley Periodicals, Inc. J Appl Polym Sci 112: 89–98, 2009

Key words: magnetic; polymer microsphere; miniemulsion polymerization

INTRODUCTION

In recent years, magnetic lattices have attracted much attention. The magnetic lattices have the advantage of rapid and easy separation of particles upon the application of an external magnetic field[1] and demonstrate potential applications in biomedical and diagnostics fields, including cellular therapy in cell labeling,[2] drug delivery,[3,4] cell separation,[5] biosensors,[6,7] immobilization of biomolecules such as oligonucleotides,[8] proteins,[9] and antibodies.[10] To successfully apply magnetic lattices to biomedical fields, it is necessary to obtain magnetic polymer particles with properties of no sedimentation,[11] near-nanosized distribution,[12] high and uniform superparamagnetic content,[13] no iron leaking, and nontoxicity.[14]

The pioneering work in synthesis of magnetic lattices has been reported by Guesdon and Avraemas[15] in 1977, who synthesized magnetic particles by the polymerization of acrylamide and agarose in the presence of iron oxide nanoparticles. Charmot[16] investigated the emulsion polymerization of styrene in the presence of organic ferrofluids. Several schemes for preparation of magnetic lattices have been reported based on the research of Charmot.

The common route to synthesize magnetic polymer particles is monomer polymerization by dispersing surface modified magnetite particles directly into the liquid phase of monomer and then initiating polymerization of the monomer in the presence of the magnetic particles. However, the magnetic polymer microspheres obtained from the conventional monomer polymerization are often incompletely and

Additional Supporting Information may be found in the online version of this article.

Correspondence to: R. Y. Hong (rhong@suda.edu.cn).

Contract grant sponsor: National Natural Science Foundation of China; contract grant numbers: NNSFC, 20876100, 20476065, 20736004.
Contract grant sponsor: Scientific Research Foundation for the ROCs of State Education Ministry.
Contract grant sponsor: State Key Lab. of Multiphase Reaction of the Chinese Academy of Science; contract grant number: 2003-5.
Contract grant sponsor: the State Key Lab. of Coal Conversion, CAS; contract grant number: 04-309.
Contract grant sponsors: Key Lab. of Organic Synthesis of Jiangsu Prov, the Chemical Experiment Center of Soochow University.
Contract grant sponsor: R and D Foundation of Nanjing Medical University; contract grant number: NY0586.

nonuniformly encapsulated, leading to the nonuniform size of resultant particles.

Because of limited polymerization methodology in the encapsulation process, new approaches have been explored and developed for the synthesis of nanosized magnetic polymer spheres, including emulsion polymerization,[17,18] miniemulsion polymerization,[19,20] emulsifier-free emulsion polymerization,[21] dispersion polymerization,[22] suspension polymerization,[23–25] and microemulsion polymerization.[26] Among these polymerization processes, miniemulsion polymerization[27–29] is considered as one of the novel polymerization methods. In the presence of coemulsifier, miniemulsion polymerization takes place inside the stable monomer droplets as reaction place in which the average diameter of monomer droplets is about 50–500 nm. Recently, a novel double miniemulsion has been developed based on the miniemulsion, and has been used to prepare polymer microspheres or nanospheres encapsulating magnetic particles. The novel method of double emulsion polymerization process is to combine the two miniemulsions to synthesize magnetite-encapsulated polymer particles. In addition, by controlling the reaction conditions, it is easier to produce monodispersed, nanoscale, and superparamagnetic polymer spheres by double miniemulsion than other methods. Gu and coworkers[30,31] had proposed a modified miniemulsion/emulsion polymerization to obtain magnetite-polystyrene (Fe_3O_4-PS) microspheres. The obtained microspheres have the particle diameter of several micrometers along with the narrow size distribution and high magnetite content.

The objective of the present investigation is to apply this double miniemulsification process for the encapsulation of magnetic particles in the poly (methyl methacrylate) (PMMA) to obtain monodispersed magnetic polymer microspheres. First, oleic acid coated magnetite particles were synthesized by coprecipitation and dispersed into octane to obtain a ferrofluid. Then the ferrofluid was miniemulsified into water using sodium dodecylsulfate (SDS) as emulsifier and hydrophobic reagent hexadecane as an osmotic agent. Furthermore, another prepared MMA miniemulsion was added into the former emulsion dropwise to carry on polymerization at 80°C. The brown magnetic emulsion was prepared. The morphology and magnetic properties of the prepared PMMA microspheres were characterized. The effects of initiator dosage and MMA concentration on PMMA conversion were investigated.

MATERIALS AND METHODS

Materials

Iron (III) chloride hexahydrate ($FeCl_3 \cdot 6H_2O$), iron (II) sulfate heptahydrate ($FeSO_4 \cdot 7H_2O$), aqueous ammonia (25%), and oleic acid were purchased from the SCRC (Sinopharm Chemical Reagent Co., Ltd.). The monomer MMA (99.5%, China National Pharmaceutical Group Corp.) was distilled under a nitrogen atmosphere with reduced pressure prior to polymerization. 2,2′-Azobis(2-isobutyronitrile) (AIBN, Shanghai Chemical Reagents Co., Ltd., China) which was used as an initiator in nonaqueous systems, was recrystallized from ethanol and then dried at room temperature in vacuum. Analytical grade Octane, chlorhydric acid, SDS (sodium dodecyl sulfate), Tween-80 (polyethylene oxide sorbitan monooleate) and Span-85 (Sorbitan trioleate) were from Shanghai Chemical Reagents Co., Ltd. and used without further purification. Hexadecane (99%) was purchased from Fluka.

Ferrofluid preparation

The preparation of ferrofluid was carried out at room temperature according to the following procedure.[32,33] First, Fe_3O_4 nanoparticles were synthesized by coprecipitation from a solution of mixture of $FeCl_3$ (0.5 M) and $FeSO_4$ (0.5 M) with a molar ratio of 1.75 : 1 using concentrated ammonia under Ar protection. Ten milliliter of ammonia aqueous solution was then quickly dropped into the solution with vigorous stirring, followed by more ammonia aqueous solution being dropped into the mixture slowly with stirring until the pH of the solution reached 9. Then, 1 g of oleic acid was added to the dispersion under vigorous stirring for 1 h at a temperature of 80°C. After that, the precipitates were collected by magnetic field separation and excess oleic acid was removed with an ethanol rinse, then the precipitate was dried in vacuum at room temperature for 12 h. Finally, the hydrophobic modified iron oxide nanoparticles were resuspended in octane at 20% (w/v). As reported by various authors,[34,35] the double bond in the hydrocarbon chain of oleic acid seems to play an important role for an effective stabilization of iron oxide in alkane medium.

Magnetic emulsion preparation

Stable (oil-in-water) magnetic emulsion was prepared by polymerization involving two miniemulsions (A and B). A typical experiment was described as follows: Miniemulsion (A) was prepared using 5 mL of ferrofluid (oleic acid coated Fe_3O_4 nanoparticles dispersed in octane with 10% (w/v) magnetite content) and 0.35 g of hydrophobic reagent hexadecane mixed in surfactant solution consisting of sodium dodecyl sulfate (SDS: 0.35 g) and distilled water (25 g). The above mixture was stirred for 0.5 h at 1300 rpm, and then adding AIBN followed by ultrasonic irradiation for 10 min in an ice-cooled bath.

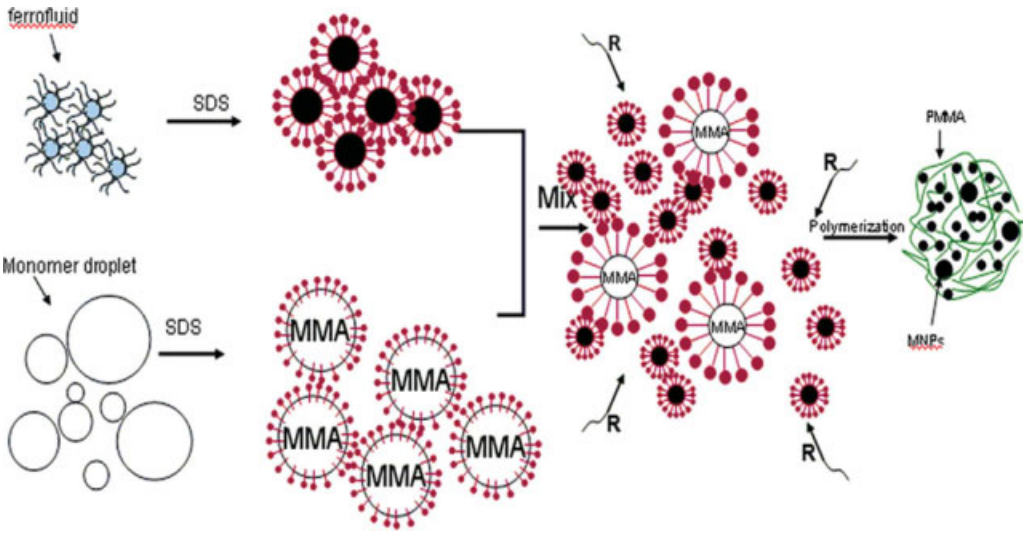

Figure 1 The reaction sketch for preparing magnetic PMMA microspheres. [Color figure can be viewed in the online issue, which is available at www.interscience.wiley.com.]

Miniemulsion (B) consisting of certain amount of MMA, 0.12 g of hexadecane, 0.12 g of SDS, 0.15 g of Tween-80 and 20 g of distilled water was prepared by magnetic stirring at ambient temperature for 1 h followed by ultrasonic irradiation for 15 min. Then Miniemulsion (A) was transferred to a 250-mL three-necked glass reactor equipped with an Ar inlet and an ordinary polytetrofluoroethyl agitator was used throughout the experiments. Miniemulsion (B) was added in portions, with intense stirring, to the Miniemulsion (A). Emulsion polymerization was carried out at 80°C with a thermal bath for 90 min. Finally, the brown magnetic emulsion was obtained. The PMMA/Fe_3O_4 magnetic microspheres can be separated from the emulsion under an external magnetic field, and can be redispersed into the emulsion with agitation. The reaction sketch map is shown in Figure 1.

Characterization

Infrared spectroscopy

Adsorption of oleic acid on the surface of magnetite particles and magnetic PMMA microspheres was examined by a Nicolet Avatar 360 Fourier transform infrared spectroscope (FTIR). Measurements were performed with pressed pellets that were made using KBr powder as diluent. Each sample (5 mg) was thoroughly mixed and crushed with 500 mg of KBr using a mortar and pestle. The mixture (80 mg) was placed in a pellet former and was pressurized for 2 min to form the KBr pellet. The FTIR spectrum was collected between the wave number of 400 and 4000 cm^{-1}.

X-ray powder diffraction

The bare and composite Fe_3O_4 nanoparticles were characterized respectively, by X-ray powder diffraction (XRD) (D/Max-IIIC, Japan) using Cu Kα radiation (λ = 1.5406 Å). Data were collected between 20° and 80°(2θ) with a step size of 0.03°(2θ) and a counting time of 100 s/step. Distances between peaks were compared with the JCDPS 5-0664 of International Center for Diffraction Data to determine crystalline structures.

Scanning and transmission electron microscopy

The size and shape of the magnetic PMMA microspheres were determined by a Hitachi H-600-II transmission electron microscope (TEM) and a Hitachi S570 scanning electron microscope (SEM). In both the cases, a drop of the dilute sample was deposited on a copper grid covered with a formvar-carbon membrane.

Thermogravimetric analysis

Perkin–Elmer TGA-7 was employed to perform the thermogravimetric analysis (TGA). Dried sample (1–5 mg) was placed in the TGA furnace and the measurements were carried out under nitrogen atmosphere with a heating rate of 15°C/min from room temperature to 600°C.

Vibrating sample magnetometer

The magnetic properties of magnetic microspheres were measured at room temperature using a BHV-55 vibrating sample magnetometer (VSM, I_{max} = 50

A, $P \leq 6$ kW, $H_{max} = 15{,}000$ Oe, sensibility between 4 and 5×10^5).

Rheological property measurements

The rheological property measurements of magnetic emulsions were carried out using a rotating rheometer (LV DV-III+, Brookfield, USA). The rotating speed range is 0.01–250 rpm, while the viscosity range of samples is from 1 cP to 2 McP. In the present investigation, a large cone spindle for low viscosity system (CPE-40, with a diameter of 48 mm and an angle degree of 0.8) and a small cone spindle for high viscosity system (CPE-52, with a diameter of 24 mm and an angle degree of 3) were employed in the measurements. The sample volume used in the tests is only 0.5 mL.

Conversion

The conversion of the emulsion polymerization was measured according to Wang et al.[36] During the emulsion polymerization, a sample of the emulsion latex was periodically taken out of the reactor, immediately poured into a weighing bottle which immersed in an ice bath to quench the reaction. The precipitated latex was dried in a vacuum oven at 50°C until constant weight. The conversion of the emulsion polymerization was calculated as follows:

$$\text{Conversion} = \frac{(W_2 - W_1) \times F \times S}{W_1 \times M_0}$$

where W_1 is the weight of the sample taken from the vessel, W_2 is the weight of dry composite polymers obtained from the sample, M_0 is the initial weight percentage of monomers (MMA) in the reaction mixture, F is the initial volume percentage of the ferrofluid in the reaction mixture, and S is the solid content of the ferrofluid (g/mL).

RESULTS AND DISCUSSION

Infrared spectroscopy

The existence of oleic acid on the surface of iron oxide particles was examined by infrared spectroscopy. The dried ferrofluid was mixed and pressed together with KBr into small tablets, as described in Section Infrared spectroscopy. Figure 2(a,b) show the FTIR spectra of Fe_3O_4 nanoparticles before and after the treatment of oleic acid, respectively. It can be seen from Figure 2(a) that the absorption band in 583 cm^{-1} is due to stretching vibration of Fe—O bond of Fe_3O_4. From Figure 2(b), when compared with untreated Fe_3O_4 nanoparticles, oleic acid treated Fe_3O_4 nanoparticles (Fig. 2) show a new adsorption at 1716 cm^{-1} corresponding to C=O groups, in addition, the peak at 955 cm^{-1} representing stretching vibration of —C=C— bond. It is indicated that the oleic acid was absorbed on the surface of magnetite particles by the reaction between the —COOH group of oleic acid and —OH group on the Fe_3O_4 surface because bare Fe_3O_4 nanoparticles and oleic acid treated Fe_3O_4 nanoparticles had been sufficiently washed by ethanol.

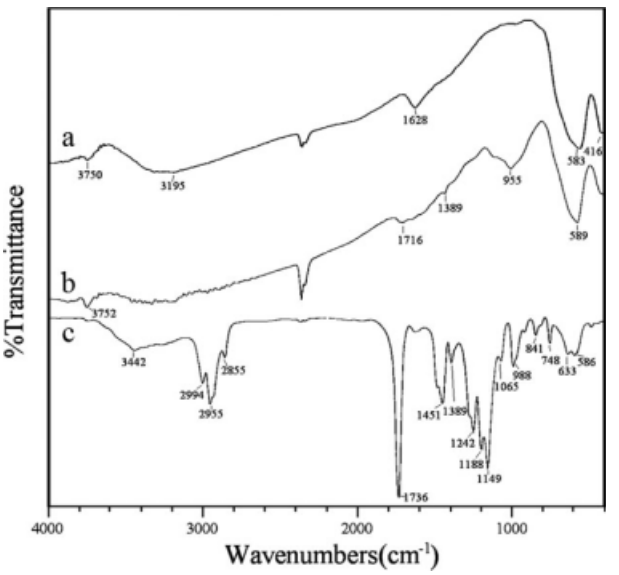

Figure 2 FTIR spectra of (a) bare Fe_3O_4 nanoparticles; (b) Fe_3O_4 nanoparticles treated by oleic acid; (c) magnetic PMMA microspheres of sample 3.

The possible chemical reaction is provided as follows:

$$Fe_3O_4(OH)_x + y\text{HOOCR} \rightarrow Fe_3O_4(OH)_{x-y}[\text{OOCR}]_y + y\text{H}_2\text{O}(\text{R}{=}{=}\text{CH}_2)_7\text{CH}{=}{=}\text{CH}(\text{CH}_2)_7\text{CH}_3)$$

The spectrum of magnetic PMMA microspheres of Sample 3 is shown in Figure 2(c). The adsorption peaks at 586.5 cm^{-1} was the characteristic absorption of Fe—O bond which confirmed the presence of Fe_3O_4 nanoparticles. A new adsorption at 1736 cm^{-1} is corresponding to C=O groups of PMMA. In addition, the bands in the 3000–2800 cm^{-1} region are attributed to the stretching of C—H bonds of the saturated alkane in PMMA, indicating the existence of PMMA. On the basis of the above analysis, the magnetite particles and PMMA were proved to be existed in the composite particles.

X-ray powder diffraction

X-ray powder diffraction patterns of bare Fe_3O_4 nanoparticles (A), oleic acid modified magnetic nanoparticles (OMP) (B), and PMMA magnetic latex particles of Sample 3 (C) are illustrated in Figure 3, respectively. It can be found in the XRD pattern of

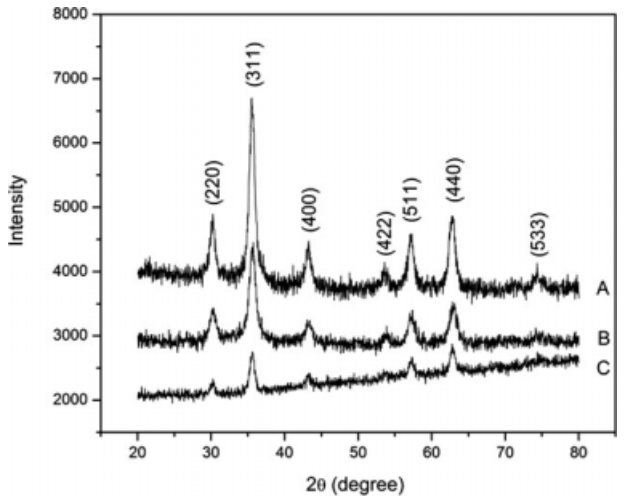

Figure 3 XRD patterns of (a) Fe_3O_4 nanoparticles; (b) Fe_3O_4 nanoparticles treated with oleic acid; (c) magnetic PMMA microspheres of sample 3.

(A) that there are a series of characteristic peaks at 2.964(220), 2.525(311), 2.092(400), 1.717(422), 1.612(511), 1.478(440), and 1.276(533). The *d* values calculated from the XRD pattern are well indexed to the inverse cubic spinel phase of Fe_3O_4. The average crystallite size *D* is calculated using the Debye-Sherrer formula $D = K\lambda/(\beta\cos\theta)$, where *K* is Sherrer constant, λ is the X-ray wavelength, β is the peak with of half-maximum, and θ is the Bragg diffraction angle. The crystallite size *D* thus obtained from this equation is found to be about 11 nm, which is basically in accordance with that from the transmission electron micrographs. From the XRD pattern of OMP (B) and PMMA microspheres (C), it was observed that the intensity of diffraction peaks was weakened, but did not disappear. The weakness of diffraction intensity of PMMA microspheres may be due to the lower content of Fe_3O_4.[37] During the synthesis process, the structure of Fe_3O_4 nanoparticles was unchanged. The results demonstrated that the Fe_3O_4 nanoparticles in PMMA microspheres have the expected crystalline structure of magnetite.

Scanning and transmission electron microscopy

In the present investigation, magnetic PMMA microspheres were obtained by double-miniemulsion polymerization and magnetic separation. The surface morphology and particle size of these microspheres were studied by TEM and SEM, as shown in Figure 4. It can be seen from the TEM images that magnetic PMMA microspheres demonstrate excellent monodispersity and all the composite particles are spherical in shape. The average diameters of the magnetic PMMA microspheres of Samples 1, 2, and 3 are 100, 120, and 150 nm, respectively. Comparing the samples of different weight ratios of MMA to OMP (Table I), it is obvious that the diameter of the microspheres increased slightly with the increasing weight ratio of MMA to OMP. Therefore, the weight ratio of MMA to OMP was an important factor in controlling the particle size of magnetic PMMA

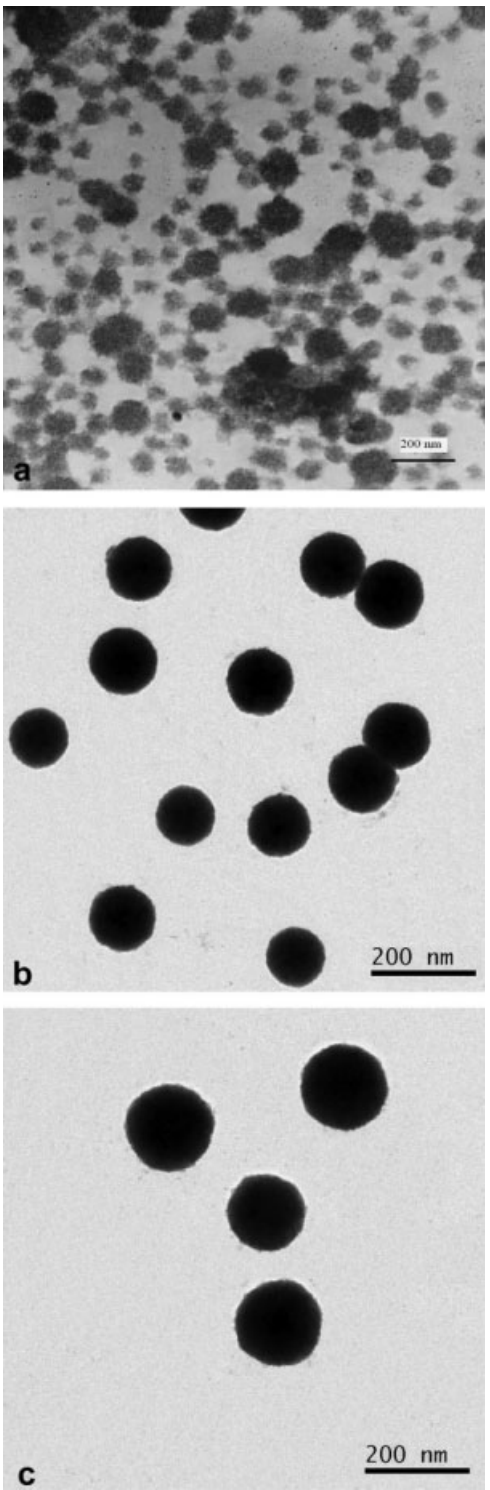

Figure 4 TEM of magnetic PMMA microspheres (a) sample 1, (b) sample 2 and (c) sample 3.

TABLE I
Synthesis Magnetic PMMA Microspheres

Sample No.	Methyl methacrylate (mg)	AIBN (mg)	Ferrofluid (mL)	Monomer : OMP (weight ratio)
1	600	6	5	6
2	900	9	5	9
3	1200	12	5	12
4	600	12	5	6
5	600	24	5	6

All experiments carry out at 80°C for 90 min.

microspheres. In addition, as observed in Figure 4(a) (Sample 1), the distribution of the magnetite nanoparticles encapsulated inside the PMMA microspheres is comparatively uniform, however, there is some OMP leaking outside the polymer spheres, while the morphology of magnetic microspheres (Samples 2 and 3) become uniform and magnetite particles seem to disperse homogeneously in the polymer spheres with the increasing weight ratio of MMA to OMP. In addition, the morphology of magnetic PMMA microspheres was studied by SEM. The SEM images of Samples 1 and 3 were shown in Figure 5(a,b). From Figure 5(a), it is apparent that OMP congregated inside microspheres, and the content of Fe_3O_4 nanoparticles in each microsphere was not consistent. Thus, the morphology of Sample 1 was not uniform and there existed flaw apparently which indicated the incomplete encapsulation of OMP. This phenomenon may be explained that the low weight ratio of MMA to OMP leads to more magnetic particles existed in the reaction system. On the other hand, the encapsulation ability of microsphere is limited, so excessive magnetic nanoparticles could not be well encapsulated by PMMA microsphere. In Figure 5(b), Although weight ratio of MMA to OMP is high, it is found that the morphology of microspheres is spherical and the OMP were dispersed homogeneously in the polymer microspheres, which reasonably matched with TEM observation [Fig. 4(c)].

Thermogravimetric analysis

The magnetite contents of the dehydrated OMP and magnetic PMMA microspheres were measured through the TGA runs under the nitrogen atmosphere at the heating rate of 15°C/min. Figure 6 illustrates the TGA curves, depicting the variations of the residual masses of the samples with the increasing temperature. The organic materials and magnetite of the samples are completely burned to generate gaseous products and converted into iron oxides at the elevated temperature (say higher than 500°C), respectively.[38] The amount of magnetite in the samples can be estimated from the residual mass percentages. Figure 6 shows that the oleic acid would completely decompose when the temperature reaches about 400°C. The TGA curve of the magnetite shows the slightly reduced weight between 25 and 100°C (2.51 wt %) that may be caused from the impurities.[39] The weight of the OMP starts to lose from 180°C and continuously decreases with the increasing temperature. About 84.32% of the overall weight loss occurs in the temperature range from 180 to 400°C and a broad endotherm peak is found at 349.62°C in the DTA corresponding to this weight-loss step and the final values of the residual mass were obtained at temperatures as low as 450°C. Thermogravimetric chart of oleic acid modified Fe_3O_4 nanoparticles pointed out that the magnetite contents of the OMP is about 87.26%.

Thermogravimetric charts of PMMA microspheres of Samples 1, 2, and 3 are shown in Figure 7(a–c), respectively. In the case of the magnetic PMMA microspheres, the loss of mass is gradual. A second endotherm peak in DTA corresponding to the

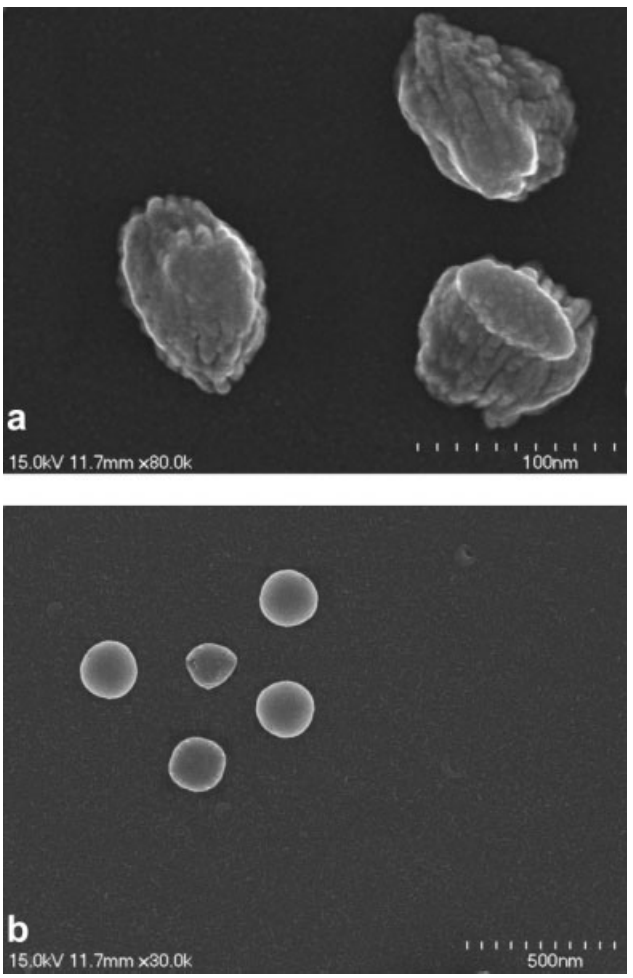

Figure 5 TEM of magnetic PMMA microspheres (a) sample 1, (b) sample 2 and (c) sample 3.

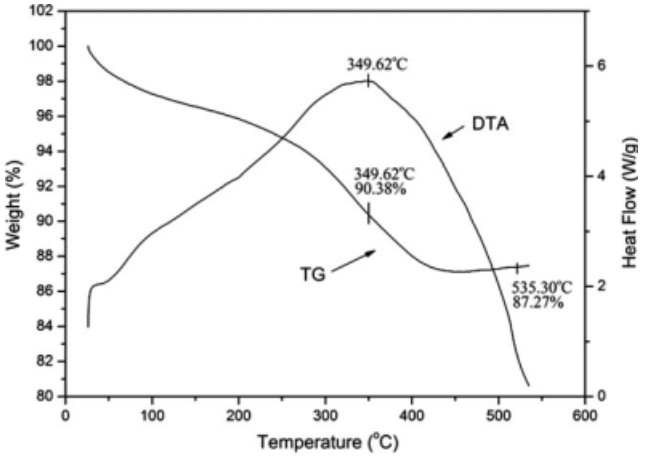

Figure 6 Weight loss curves of oleic acid modified Fe_3O_4 nanoparticles.

PMMA degradation was clearly observed around 400°C for the magnetic latex and could reach the final values of the residual mass were obtained at temperatures as low as 500°C, revealing the complete decomposition of PMMA. The magnetic PMMA microspheres with higher weight ratio of MMA to OMP would have the smaller percentage of the residual mass. In Figure 7, the measured magnetite contents of the magnetic PMMA microspheres are 26.78, 17.96, and 16.53 wt % with respect to the weight ratios of MMA to OMP of 8, 10, and 12. It is observed that the actual magnetite content of the PMMA particles is larger than the value calculated from the applied weight ratio of MMA to OMP which is due to that the MMA with the solubility of 15 g/L (20°C) would partially dissolve in the water phase. Thus some nonmagnetic PMMA particles are generated simultaneously.

Magnetic properties of magnetite nanoparticles

The magnetic properties of oleic-acid-coated magnetite particles and magnetic PMMA microspheres were characterized by a vibrating sample magnetometer (VSM). Figure 8 shows the typical room-temperature magnetization curves of bare Fe_3O_4, OMP and magnetic PMMA microspheres of Sample 3, respectively. As shown in this figure, the saturation magnetization of bare Fe_3O_4 nanoparticles is 65.6 emu/g and oleic acid coated magnetite particles is 47.7 emu/g. For the magnetic PMMA microspheres, the saturation magnetization is 23.7 emu/g. All the samples show a typical superparamagnetic behavior. However, the saturation magnetization of the nanoparticles was significantly smaller than that of bulk magnetite, which is 84 emu/g.[40] The lower saturation magnetization can be ascribed to the rather small size of the magnetite nanoparticles and the mass of the added oleic acid on the particles.[41] In addition, low saturation magnetization of magnetic PMMA microspheres may be attributed large part to the oxidation during the polymerization, which leads to the formation of some nonmagnetic iron oxide (Fe_2O_3).

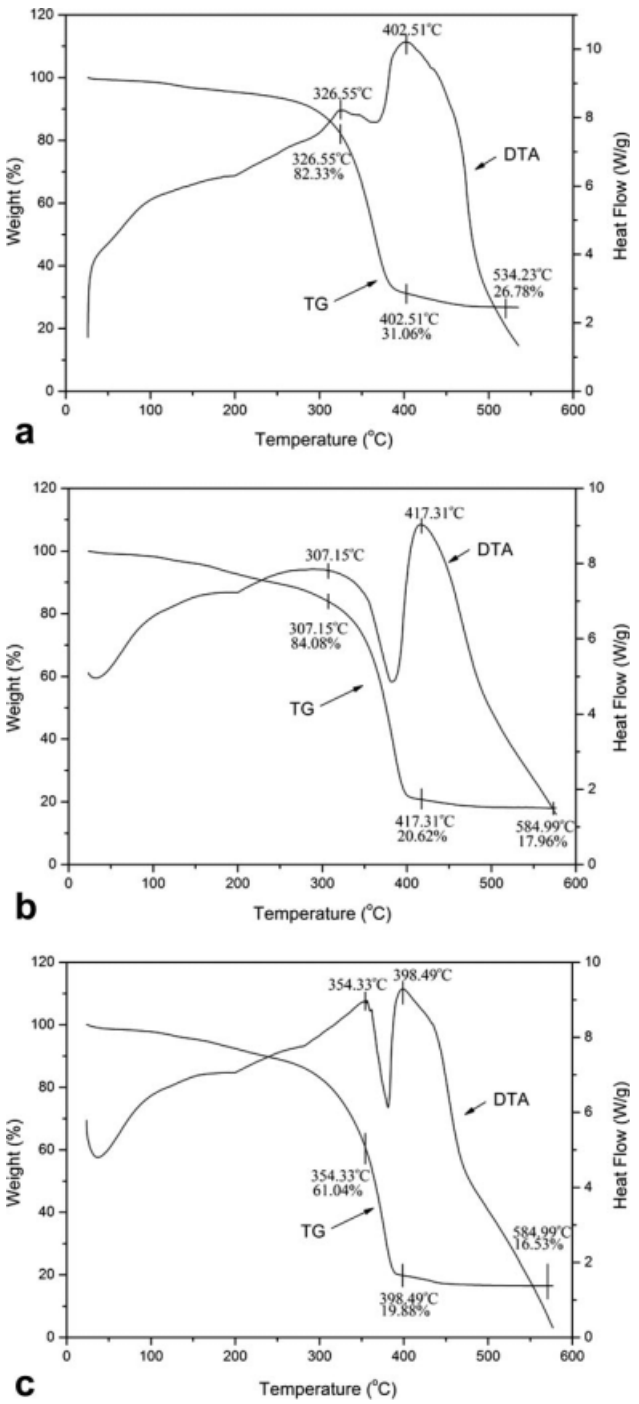

Figure 7 Weight loss curves of PMMA microspheres with various weight rations of MMA/OMP of (a) sample 1, (b) sample 2, (c) sample 3.

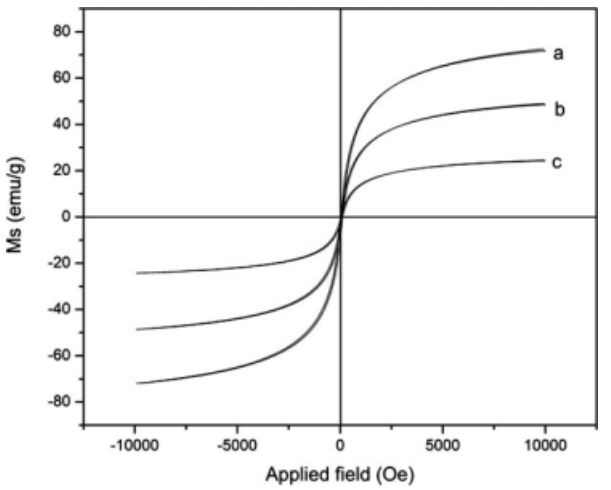

Figure 8 Magnetization curves obtained by VSM at room temperature of (a) Fe_3O_4 nanoparticles; (b) oleic-acid-coated magnetite; and (c) magnetic PMMA microspheres of sample 3.

Efforts of reaction conditions

The effects of initiator dosage and MMA concentration on PMMA conversion were investigated respectively, as follows.

Initiator dosage

The effect of the initiator dosage on PMMA conversion with fixed amount of MMA was shown in Figure 9. Comparing the plots of different initiator dosages, the reaction rate is in the following order: 24 mg AIBN > 12 mg AIBN > 6 mg AIBN. It is apparent that the polymerization rate was higher under the condition of a higher initiator concentration. Higher amount of the initiator could increase the polymerization of MMA in the emulsion. However, when the concentration of initiator exceeded 50 mg, the excessive amount of the initiator could initiate the polymerization of MMA in the solution which leads to the production of nonmagnetic PMMA. In addition, the reason for the conversion of less than 100% was due to the glassy effect.[36] When the glass-transition temperature of the polymer particles (T_g of magnetic PMMA particles of Sample 3 is 108.16°C, as shown in the Supplementary material) was higher than the reaction temperature (80°C), the monomer propagation was difficult to continue in the polymer particles; thus, the final conversion could not reach 100%.

MMA monomer concentration

The effect of MMA monomer concentration on MMA conversion was investigated, and the result was shown in Figure 9. Comparing the plots of different MMA monomer concentrations, the reaction rate is in the following order: 6 g MMA > 9 g MMA > 12 g MMA. As Wang et al.[36] reported, with a lower concentration of MMA in the polymerization system, the ferrofluid acted as the seeds in the polymerization and the reaction rate was very fast. When the concentration of MMA increased, the reaction rate slowed down. It can be explained that most of the layer structure of the surfactant of the ferrofluid was destroyed by the excess monomer and then the polymerization was mostly initiated by self-nucleation.[17]

Rheological property of magnetic emulsion

Viscosity versus time

Figure 10 shows the viscosities of magnetic emulsions of different MMA concentrations at a fixed

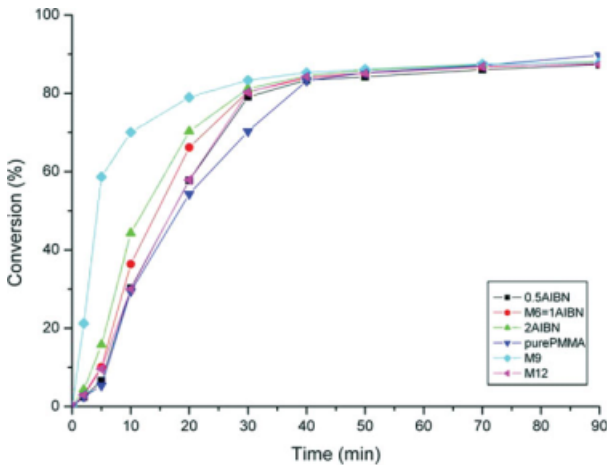

Figure 9 Conversion versus time of emulsion polymerization at different initiator dosages. [Color figure can be viewed in the online issue, which is available at www.interscience.wiley.com.]

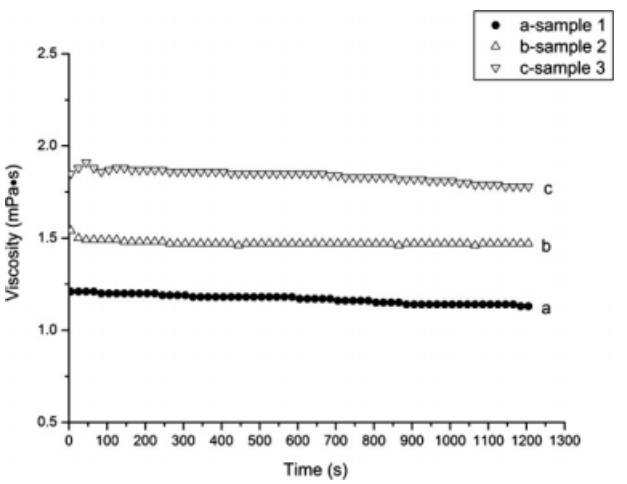

Figure 10 Time evolution of magnetic emulsion viscosity with different samples: (a) sample 1; (b) sample 2; (c) sample 3.

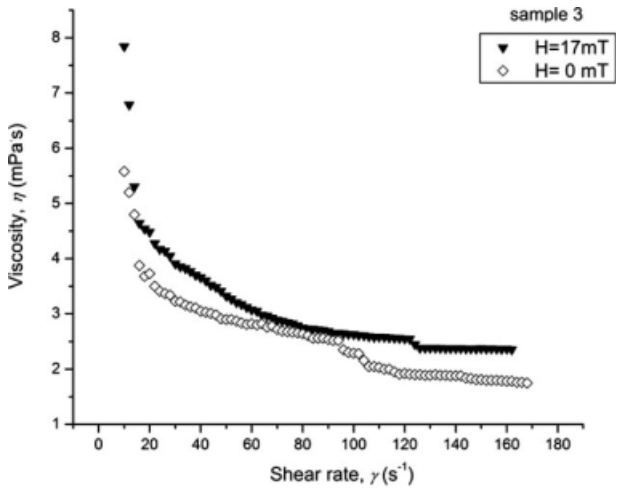

Figure 11 Viscosity versus shear rate of magnetic emulsion (sample 3) with and without magnetic field.

shear rate (140 s^{-1}). We can see from the figure that the viscosity of magnetic emulsions do not change with the shearing time at the constant shear rate and the viscosity basically keeps constant which indicated the magnetic emulsions were stable. When the magnetic emulsions were moved with the rotor, the PMMA coated solid particles also rotated with the rotor which lead to the destruction of magnetic latex structures at steady state. Because the solid content of magnetic emulsions is below 20% and the concentration of magnetic PMMA particles was low, the entanglement of polymer chains will not happen. This can be explained why the viscosity of magnetic emulsion does not change with the shear time.

Viscosity with/without magnetic field

In this section, the magnetic field with the intensity of $H = 17$ mT was applied to the magnetic emulsions between the spindle and cup of the rotating rheometer. The intensity of magnetic field was measured using a Hall-effect sensor. The viscosities of magnetic emulsions with and without magnetic field were illustrated in Figure 11. By comparing the curves, it is found that the applied magnetic field had obvious effects on the viscosity of magnetic emulsion. Because the viscosity of water cannot respond to the applied magnetic field, the viscosity of the magnetic emulsion is determined by the properties and contents of the magnetic PMMA particles. Under magnetic field, the magnetic PMMA particles were polarized and arranged their orientation along the direction of the magnetic field, also the interaction among the magnetic PMMA particles was enhanced. Therefore, the flow resistance increased. Finally, it gave higher viscosity of the emulsion. In addition, it is observed that there is an abrupt change of viscosity at the shear rate of 125 and 90 s^{-1} for magnetic emulsions with and without magnetic field, respectively. This phenomenon may be due to the destruction of microstructures of magnetic emulsion at high hear stress.[42] With the increasing shear rate, these microstructures of magnetic emulsions would be destroyed gradually under the shear stress which may cause an abrupt change of viscosity when shear stress reaches some extent. However, the applied magnetic field can also rearrange the magnetic nanoparticles, leading to the formation of orderly microstructures.[43] So the viscosity of magnetic emulsion under magnetic field had an abrupt change at higher shear rate than that without magnetic field.

CONCLUSIONS

Magnetic PMMA microspheres were successfully prepared by double miniemulsion polymerization. The product was characterized by XRD, TEM, FTIR, TGA, and VSM. The following conclusions can be drawn in the present investigation: (1) FTIR indicates that the Fe_3O_4 nanoparticles and PMMA exist in the composite particles. XRD result shows that PMMA microspheres have the expected crystalline structure of magnetite. (2) The size of the magnetic PMMA microspheres is between 100 and 150 nm from TEM observation. The weight ratio of monomers to OMP plays an important role in controlling the morphology of magnetic composite particles. The particle diameter increases with the increasing weight ratio of MMA to OMP. (3) TG curve indicates that magnetite content of microspheres is between 15 and 26 wt %, depending on the amount of Fe_3O_4 nanoparticles. The produced magnetic polymer microspheres were superparamagnetic with the saturation magnetization of 24.1 emu/g. (4) Studies on the effect of AIBN initiator and MMA monomer dosages on the polymerization behavior in the presence of magnetite particles reveals that high amount of the initiator and low concentration of MMA leads to a much faster polymerization. (5) Rheological measurements of magnetic emulsion reveal that the viscosity of magnetic emulsion is constant at a fixed shear rate, and the applied magnetic field has obvious effect on the viscosity of the emulsion.

References

1. Olsvik, O.; Popovic, T.; Skjerve, E.; Cudjoe, K. S.; Hornes, E.; Ugelstad, J.; Uhlen, M. Clin Microbiol Rev 1994, 7, 43.
2. Ito, A.; Honda, H.; Kobayashi, T. Cancer Immun Immunother 2005, 55, 320.
3. Goodwin, S.; Peterson, C.; Hoh, C.; Bittner, C. J Magn Magn Mater 1999, 194, 132.
4. Morales, M. P.; Miguel, O. B.; Alejo, R. P.; Cabello, J. R.; Verdaguer, S. V.; O'Grady, K. J Magn Magn Mater 2003, 266, 102.
5. Arshady, R. Biomaterials 1993, 14, 5.

6. Hiergeist, R.; Andrä, W.; Buske, N.; Hergt, R.; Hilger, I.; Richter, U.; Kaiser, W. J Magn Magn Mater 1999, 201, 420.
7. Astalan, A. P.; Ahrentorp, F.; Johansson, C.; Larsson, K.; Krozer, A. Biosens Bioelectron 2004, 19, 945.
8. Ganachaud, F.; Elaissari, A.; Pichot, C.; Laayoun, A.; Cros, P. Langmuir 1997, 13, 701.
9. Revilla, J.; Elaissari, A.; Carriere, P.; Pichot, C. J Colloid Interface Sci 1996, 180, 405.
10. Delair, T.; Pichot, C.; Mandrand, B. Colloid Polym Sci 1994, 272, 72.
11. Wang, P.; Lee, C.; Young, T. J Polym Sci Part A: Polym Chem 2005, 43, 1342.
12. Shchukin, D. G.; Radtchenko, I. L.; Sukhorukov, G. B. Mater Lett 2003, 57, 1743.
13. Wilhelm, C.; Billotey, C.; Roger, J.; Pons, J. N.; Bacri, J. C.; Gazeau, F. Biomaterials 2003, 24, 1001.
14. Panyam, J.; Labhasetwar, V. Adv Drug Deliv Rev 2003, 55, 329.
15. Guesdon, J. L.; Avraemas, S. Immunochemistry 1977, 14, 443.
16. Charmot, D. Prog Colloid Polym Sci 1989, 76, 94.
17. Montagne, F.; Monval, O. M.; Pichot, C.; Elaissari, A. J Polym Sci Part A: Polym Chem 2006, 44, 2642.
18. Horák, D.; Chekina, N. J Appl Polym Sci 2006, 102, 4348.
19. Qiu, G. H.; Wang, Q.; Wang, C.; Lau, W. L.; Guo, Y. L. Ultrason Sonochem 2007, 14, 55.
20. Zhang, Q. Y.; Xie, G.; Zhang, H. P.; Zhang, J. P.; He, M. J Appl Polym Sci 2007, 105, 3525.
21. Wang, P. H.; Pan, C. Y. J Appl Polym Sci 2000, 75, 1693.
22. Horák, D. J Polym Sci Polym Chem 2001, 39, 3707.
23. Maria, L. C. S.; Leite, M. C. A. M.; Costa, M. A. S.; Ribeiro, J. M. S.; Senna, L. F.; Silva, M. R. Mater Lett 2004, 58, 3001.
24. Ma, Z. Y.; Guan, Y. P.; Liu, X. Q.; Liu, H. Z. J Appl Polym Sci 2005, 96, 2174.
25. Lee, Y. H.; Rho, J. H.; Jung, B. S. J Appl Polym Sci 2003, 89, 2058.
26. Zaitsev, V. S.; Filimonow, D. S.; Presnyakov, I. A.; Gambino, R. J.; Chu, B. J. J Colloid Interf Sci 1999, 212, 49.
27. Antonoett, M.; Landfester, K. Prog Polym Sci 2002, 27, 689.
28. Asua, J. M. Prog Polym Sci 2002, 27, 1283.
29. Tiarks, F.; Landfester, K.; Antonietti, M. Chem Phys 2001, 202, 51.
30. Xu, H.; Cui, L. L.; Tong, N. H.; Gu, H. C. J Am Chem Soc 2006, 128, 15582.
31. Cui, L. L.; Gu, H. C.; Xu, H.; Shi, D. L. Mater Lett 2006, 60, 2929.
32. Hong, R. Y.; Li, J. H.; Li, H. Z.; Ding, J.; Zheng, Y.; Wei, D. G. J Magn Magn Mater 2008, 320, 1605.
33. Hong, R. Y.; Pan, T. T.; Han, Y. P.; Zhang, S. Z.; Li, H. Z.; Ding, J. J Appl Polym Sci 2007, 106, 1439.
34. Wooding, A.; Kilner, M.; Lambrick, D. B. J Colloid Interface Sci 1991, 144, 236.
35. Tadmor, R.; Rosenweig, R. E.; Frey, J.; Klein, J. Langmuir 2000, 16, 9117.
36. Wang, P. C.; Chiu, W. Y.; Lee, C. F.; Young, T. H. J Polym Sci Part A: Polym Chem 2004, 42, 5695.
37. Yamaura, M.; Camilo, R. L.; Sampaio, L. C.; Macêdo, M. A.; Nakamura, M.; Toma, H. E. J Magn Magn Mater 2004, 279, 210.
38. Zheng, W.; Gao, F.; Gu, H. J Magn Magn Mater 2005, 288, 403.
39. Baechler, S. M. R.; Cortés, S. L. G.; Orozco, J.; Sagredo, V.; Fontal, B.; Mora, A.J.; Delgado, G. Mater Lett 2004, 58, 2447.
40. O'Handley, R. C. Modern Magnetic Materials: Principles and Applications; Wiley: New York, 2000.
41. Goya, G. F.; Berquo, T. S.; Fonseca, F. C. J Appl Phys 2003, 94, 3520.
42. Hong, R. Y.; Ren, Z. Q.; Han, Y. P.; Li, H. Z.; Zheng, Y.; Ding, J. Chem Eng Sci 2007, 62, 5912.
43. Han, Y. P.; Hong, R. Y.; Wang, L. S.; Ding, J. J Cent South Univ Technol 2007, 6, 124.